Electronic Supplementary Material (ESI) for Chemical Communications.

Supplementary information

An exotic band structure of a supramolecular honeycomb lattice formed by a pancake π-π interaction between triradical trianions of triptycene tribenzoquinone

Yoshiaki Shuku,[a] Asato Mizuno,[a] Ryo Ushiroguchi,[a] Chang Seok Hyun,[b] Young Jun Ryu,[b] Byeong-Kwan An,[b] Ji Eon Kwon,[c] Soo Young Park,[c] Masahisa Tsuchiizu,[d] Kunio Awaga[a*]

[a] Department of Chemistry, Nagoya University, Furo-cho, Chikusa-ku, Nagoya 464-8602, Japan

[b] Department of Chemistry, The Catholic University of Korea, 43 Jibong-ro, Wonmi-gu, Bucheon, Gyeonggi-do, 14662, Korea

[c] Center for Supramolecular Optoelectronic Materials (CSOM), Research Institute of Advanced Materials (RIAM), Department of Materials Science and Engineering, Seoul National University, 1 Gwanak-ro, Gwanak-gu, Seoul 08826, Korea

[d] Department of Physics, Nara Women's University, Kitauoyanishi-machi, Nara 630-8506, Japan

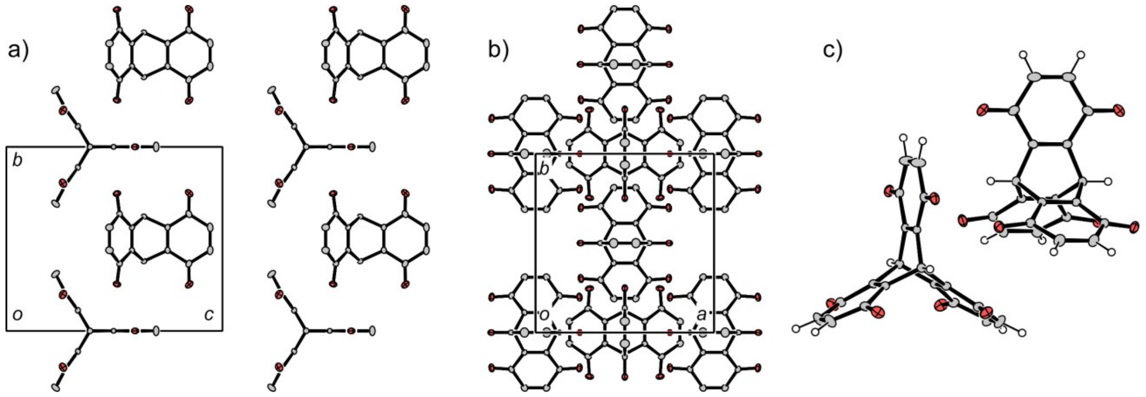

Figure S1. Crystal structure of neutral TT viewed along *a* axis (a) and *c* axis (b). Arrangement of nearest neighboring molecules in neutral TT crystal structure (c).

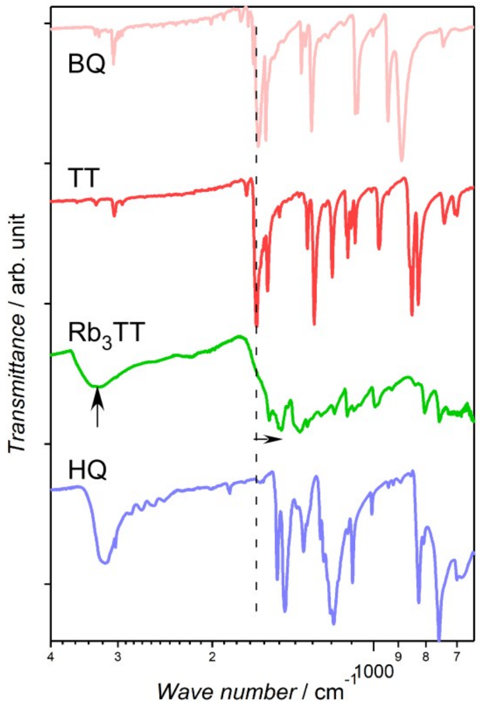

Figure S2. IR spectra of BQ, neutral TT, Rb_3TT and hydroquinone (HQ).

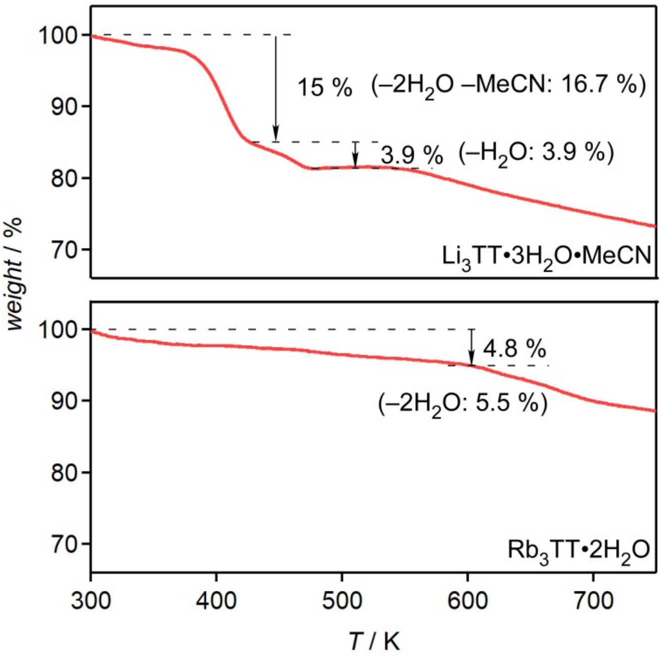

Figure S3. TG analysis of $Li_3TT•3H_2O•CH_3CN$ and $Rb_3TT•2H_2O$. Observed weight losses are shown next to the arrows. Expected molecules for the weight loss and their weight ratios in the crystal structures are shown in the parentheses.

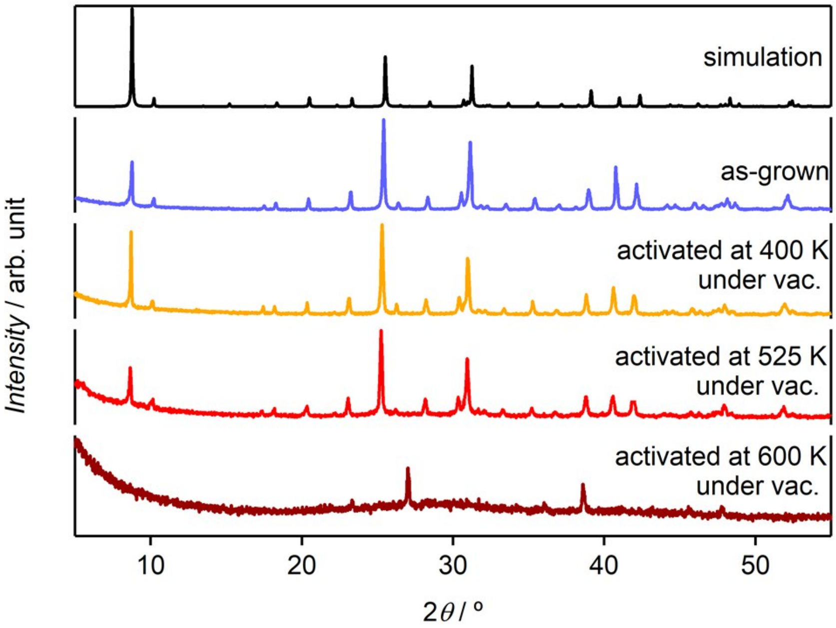

Figure S4. Simulated and experimental PXRD patterns for the $Rb_3TT•2H_2O$. XRD patterns were simulated using the single crystal structure and were measured on as-grown crystals and the crystals after being heated at various temperatures under vacuum.

Table S1. Selected bond lengths (Å) of neutral and anionic TT.

bond	a	b	c	d	e
TT	1.223(3)	1.474(3)	1.471(4)	1.343(3)	1.345(5)
	1.219(2)	1.471(2)	1.482(3)	1.344(2)	1.340(3)
Li$_3$TT	1.281(4)	1.447(3)	1.440(4)	1.359(4)	1.371(4)
	1.275(4)	1.442(4)	1.445(3)		
	1.273(3)	1.445(4)	1.446(4)	1.353(4)	1.364(4)
	1.274(3)	1.448(3)	1.437(4)		
	1.287(4)	1.444(3)	1.442(3)	1.362(4)	1.366(4)
	1.287(4)	1.444(3)	1.434(3)		
Rb$_3$TT	1.272(3)	1.437(3)	1.445(3)	1.370(3)	1.369(3)

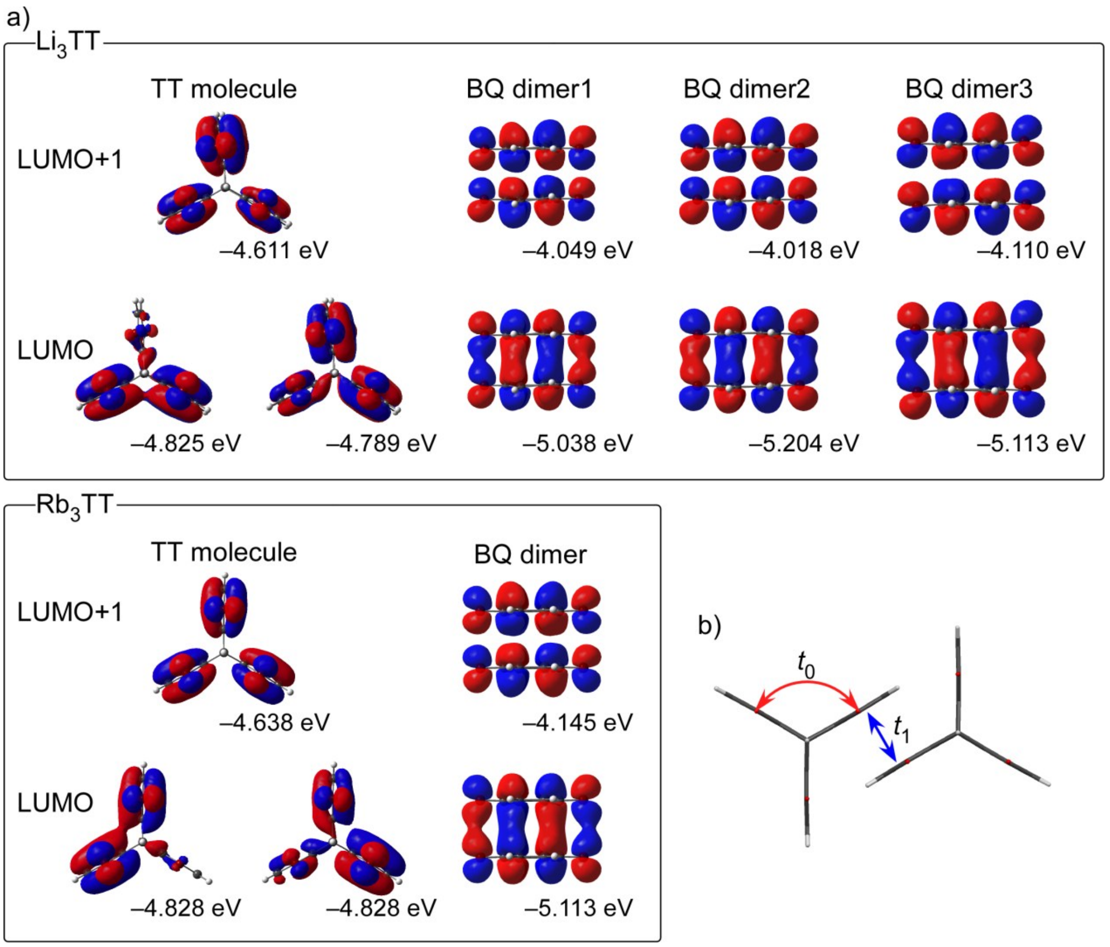

Figure S5. a) The LUMO and LUMO+1 orbitals of TT and BQ dimer with their MO energies. b) The definition of the transfer integrals t_0 and t_1.

Table S2. The parameters obtained by the DFT calculations for TT molecules and BQ dimers in Li_3TT and Rb_3TT. MO energies of LUMO (averaged for the TT molecule of the Li salt) and LUMO+1 of TT molecules and BQ dimers (E_{LUMO} and $E_{\mathrm{LUMO+1}}$), their energy differences (ΔE) and the estimated transfer integrals (t).

	E_{LUMO} / eV	$E_{\mathrm{LUMO+1}}$ / eV	ΔE / eV	t / eV
TT (Li)	−4.807	−4.611	0.196	−0.065
BQ dimer (Li)	−5.038	−4.049	0.989	−0.495
	−5.204	−4.018	1.186	−0.593
	−5.113	−4.110	1.003	−0.502
TT (Rb)	−4.828	−4.638	0.190	−0.063
BQ dimer (Rb)	−5.113	−4.145	0.968	−0.484

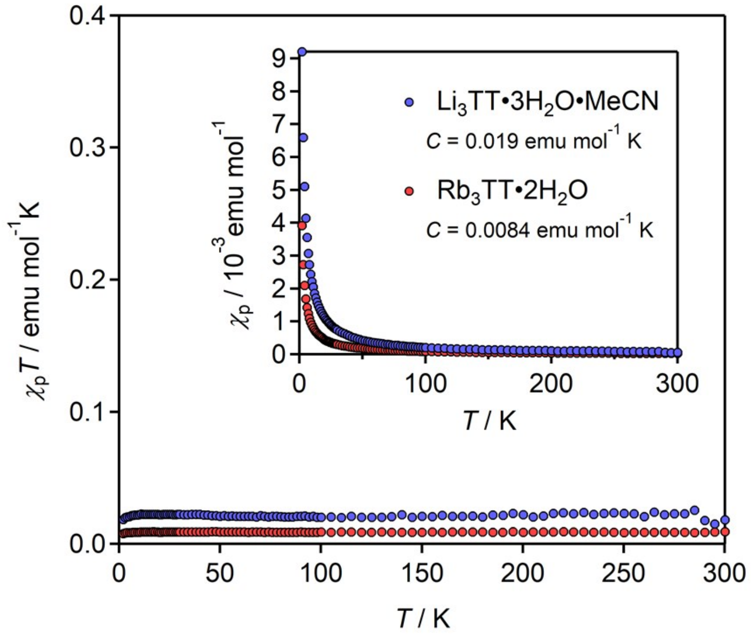

Figure S6. Temperature dependences of χ_pT and χ_p (insert) for $Li_3TT•3H_2O•CH_3CN$ (blue) and $Rb_3TT•2H_2O$ (red).

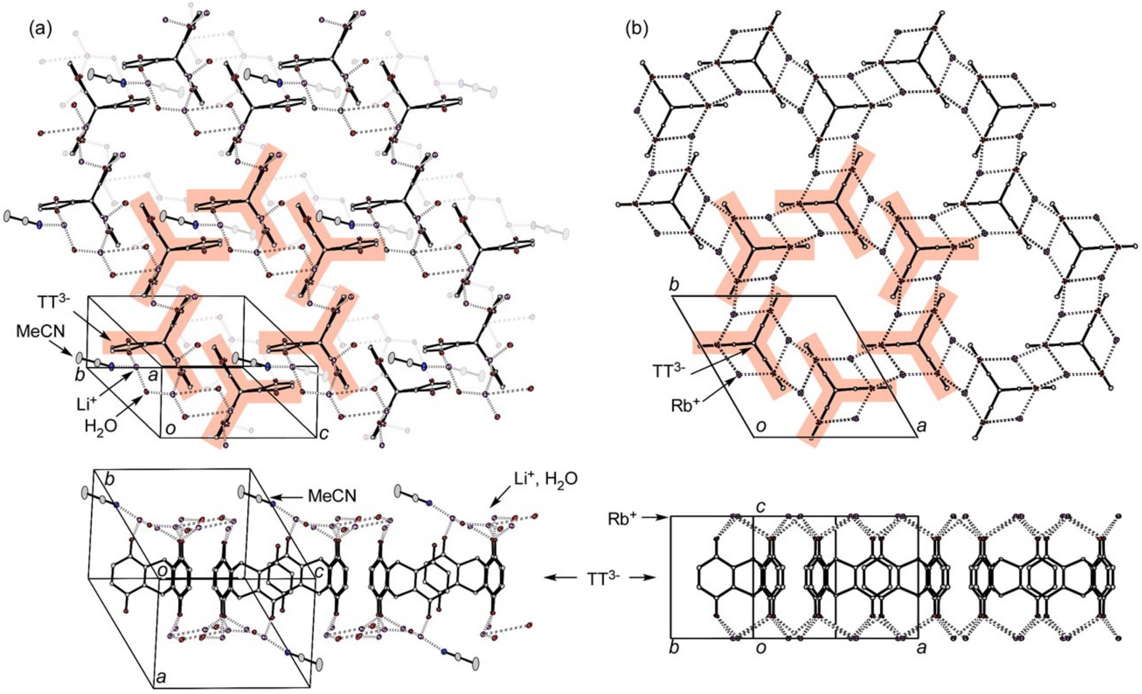

Figure S7. Crystal structures of $Li_3TT•3H_2O•CH_3CN$ (a) and $Rb_3TT•2H_2O$ (b).

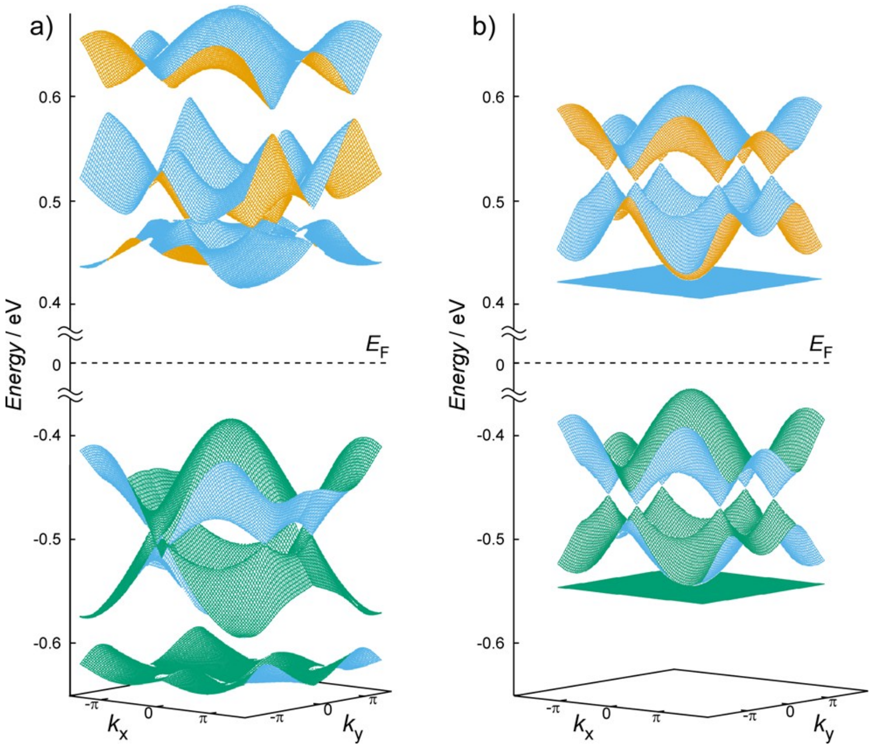

Figure S8. Band structures of $Li_3TT•3H_2O•CH_3CN$ (a) and $Rb_3TT•2H_2O$ (b).

Experimental Details

General Procedures

All the chemicals were used as purchased. During the crystallization of the anion radical salts, the cells were kept under N_2 atmosphere, and the solvent was purged with N_2 before use. $RbClO_4$ was prepared by the reaction between water solutions of RbCl and $HClO_4$, and obtained colorless powder was washed by water. ***Caution!*** *Although no problem was encountered in this work, perchlorate salts are potentially explosive and they should be handled with care.*

Electrochemical measurements

Cyclic voltammetry was performed using a Hokuto Denko HZ-5000 Automatic Polarization System at room temperature. A conventional three-electrode cell was used, which consisted of a glassy carbon disk (3 mm diameter) as the working electrode, a Pt wire as the counter electrode and Ag /Ag^+ (a solution of 0.01M $AgNO_3$ and 0.1 M n-Bu_4NClO_4 in CH_3CN) as the reference electrode. Solutions were deoxygenated by passing dry nitrogen through the solution before measurements. Ferrocene was used as an internal standard, and the potential has been converted to the ferrocene scale.

Thermogravimetric measurements

Thermogravimetric (TG) analysis was performed on a SII Exstar 6000 TG/DTA 6200 (Seiko) instrument at a heating rate of 5 ˚C/min under nitrogen atmosphere. Crystals of $Li_3TT•3H_2O•CH_3CN$ (1.939 mg) and $Rb_3TT•2H_2O$ (1.997 mg) were used as a sample. In contrast to the quick weight loss of $Li_3TT•3H_2O•CH_3CN$ at 380 K, $Rb_3TT•2H_2O$ shows gradual weight loss up to decomposition temperature (~590 K) which may be due to the strong disorder of water molecules without specific interactions to the honeycomb lattice or cation layer.

Powder X-ray measurements

Powder X-ray measurements were performed using a Rigaku Multiflex X-ray diffractometer with Cu Kα radiation (λ = 1.54 Å) under ambient conditions. As grown crystals of $Rb_3TT•2H_2O$ and the crystals after being heated at 400 K, 525 K and 600 K under vacuum were used as samples. Theoretical powder patterns were calculated on the basis of the single crystal structure.

Single crystal X-ray structural analyses

Single crystal X-ray investigations were performed at 123 K. Crystals were mounted on a loop using oil (CryoLoop, Immersion Oil, Type B; Hampton Research Corp.) and set on a Rigaku RA-Micro007 with a Saturn CCD detector by using graphite-monochromated Mo Kα radiation (λ = 0.71075 Å) under a cold nitrogen stream. The frame data were integrated and corrected for absorption with the Rigaku/MSC CrystalClear package.[S1] The structures were solved by direct methods[S2] and standard difference map techniques, and were refined with full-matrix least-square procedures on F^2 by a Rigaku/MSC CrystalStructure package. [S3] Anisotropic refinement was applied to all non-hydrogen atoms. Hydrogen atoms for water molecule in $Li_3TT•3H_2O•CH_3CN$ were located in a difference Fourier map and refined isotropically and the other hydrogen atoms were placed at calculated positions and refined using a riding model. The electron densities in the 1D pore were flattened, using the SQUEEZE subroutine of PLATON,[S4] and only the 2D honeycomb network structure of the TT anions and the Rb ions coordinating to the oxygen atoms of TT, were refined. CCDC 1816744-1816746 contain the supplementary crystallographic data for this paper. This data can be obtained free of charge from The Cambridge Crystallographic Data Centre via www.ccdc.cam.ac.uk/data_request/cif.

Magnetic measurements

Magnetic susceptibility measurements were carried out on polycrystalline samples on a MPMS-XL Quantum Design magnetometer. All of the measurements used a plastic straw as the sample folder. Measurements were performed under 0.5 T in the temperature range of 2–300 K. The temperature dependences of the paramagnetic susceptibilities χ_P of the anion radical salts were calculated with experimentally obtained diamagnetic susceptibilities by assuming the magnetic contribution follow the Curie law.

Computational Details

The calculations was performed using the Gaussian09W program package.[S5] The molecular structure of TT was optimized using B3LYP methods with 6-311+G(d) basis sets.

We estimated the intramolecular (t_0) and intermolecular (t_1) transfer integrals (Figure S5) by DFT calculations. The single point energy calculations for a neutral TT and a neutral dimer of BQ units were carried out using the B3LYP methods with 6-311+G(d) basis set. The geometry of the TT and BQ dimer for the calculations were taken from the crystal structure of the Li and Rb salts of TT radical anion. These calculations were performed with the Gaussian09 package. The energy difference (ΔE) between the LUMO and LUMO+1 for TT correspond to $3t_0$ and the ΔE between LUMO and LUMO+1 for BQ dimer corresponds $2t_1$ (Table S2). The band structure calculation was carried out by the tight-binding approximation taking into account single t_0 and three different t_1 for Li salt and single t_0 and single t_1 for Rb salt, and setting the charge of TT as −3.

IR spectroscopy

IR spectra were measured on a Perkin Elmer Spectrum One FT-IR Spectrometer in ATR mode.

Preparation and crystallization of TT and its radical anion salts

9,10-Dihydro-9,10[1',2']-Benzenoanthracene-1,4,5,8,13,16-hexone (TT): TT was prepared by the literature method,[S6,21] and the final product was further purified by flash chromatography on silica gel using ethyl acetate: dichloromethane (1:30) as an eluent. ^{1}H-NMR (500 MHz, $CDCl_3$) δ(ppm)

6.70 (s, 6H), 6.60 (s, 2H); IR (*v,* cm^{-1}) 1650 (C=O stretching); MS (EI) m/z: calcd for $C_{20}H_8O_6$ 344.03, found 344.00 (M)$^+$; Anal. Calcd for $C_{20}H_8O_6$: C, 69.78; H, 2.34 O, 27.88. Found: C, 69.50; H, 2.23; O, 28.23. Yellow block crystals for the structural analysis were obtained by vacuum sublimation at 200 ˚C under 50 ml/s N_2 flow. Though the crystal structure has been reported,[21] we reinvestigated single crystal X-ray structural analysis at lower temperature (123 K). Crystal data: $C_{20}H_8O_6$; Tetragonal; $I4_1md$ (#109), a = 10.781(3), c = 12.687(3) Å; V = 1474.6(6) Å^3; Z = 4; T = 123 K; Final R_1 = 0.0275 ($I > 2\sigma(I)$), wR_2 = 0.0735 (all data), GOF = 1.134.

Li_3TT•3H_2O•CH_3CN: Crystals of Li_3TT•3H_2O•CH_3CN were obtained by the slow diffusion method between TT (10 mg) and excess amount of LiI (~50 mg). A glass tube with TT in and LiI were placed in a 10 ml vial to keep reactants apart. To the vial, acetonitrile with a small drop of water were poured above the glass tube end. After 1 week, shiny red platelet crystals had grown in brown solution. Crystal data: $C_{22}H_{17}Li_3NO_9$; Triclinic; $P\bar{1}$ (#2); a = 9.739(5), b = 10.881(6), c = 11.611(6) Å; α = 116.488(6), β = 92.9867(14), γ = 110.107(5) ˚; V = 1002.8(8) Å^3; Z = 2; T = 123 K; Final R_1 = 0.0527 ($I > 2\sigma(I)$), wR_2 = 0.1300 (all data), GOF = 1.074.

Rb_3TT•2H_2O: Crystals of Rb_3TT were obtained by galvanostatic electrocrystallization (0.5 μA) of a saturated $RbClO_4$ electrolyte solution of acetonitrile containing 1 mM of TT and a small drop of water. After 1 week, black needle-shaped crystals had grown. Crystal data: $C_{20}H_8O_6Rb_3$; Hexagonal; $P6/m$ (#175), a = 11.6406(19), c = 8.6575(14) Å; V = 1016.0(3) Å^3; Z = 2; T = 123 K; Final R_1 = 0.0249 ($I > 2\sigma(I)$), wR_2 = 0.0621 (all data), GOF = 1.119.

In the X-ray structural analysis, the structure in this 1D cavity could not refined due to disordering, so that we flattened the electron density in it, which corresponded to 39 electrons in the unit cell, by using the SQUEEZE program of PLATON. IR spectrum of the Rb salt shows a broad band in the region of OH (~3200 cm^{-1}) stretching mode, which suggests the inclusion of H_2O molecules as a crystal solvent (Figure S2). The IR spectrum also shows the very weak signal around 2200 cm^{-1} which indicates the existence of the trace amount of acetonitrile molecules in the crystal. Assuming that water is the only major crystal solvent molecule in the cavity, the electron density in the cavity can be well explained by the chemical formula, Rb_3TT•2H_2O, which means four water molecules (40 electrons) in the unit cell.

Table S3. Crystallographic data for neutral TT and anionic salts of TT.

	TT	$Li_3TT \bullet 3H_2O \bullet CH_3CN$	Rb_3TT
Formula	$C_{20}H_8O_6$	$C_{22}H_{17}Li_3NO_9$	$C_{20}H_8O_6Rb_3$
Formula weight / g mol^{-1}	344.28	460.20	600.68
Temperature / K	123	123	123
Crystal dimensions / mm^3	0.09 × 0.08 ×0.07	0.06 × 0.04 ×0.03	0.18 × 0.02 ×0.01
System	Tetragonal	Triclinic	Hexagonal
Space group	$I4_1md$ (#109)	$P\bar{1}$ (#2)	$P6/m$ (#175)
a / Å	10.781(3)	9.739(5)	11.6406(16)
b / Å		10.881(6)	
c / Å	12.687(3)	11.611(6)	8.6575(14)
α / °		116.488(6)	
β / °		92.9867(14)	
γ / °		110.107(5)	
V / Å^3	1474.6(6)	1002.8(8)	1016.0(3)
Z	4	2	2
ρ_{calcd} / g cm^{-3}	1.551	1.524	1.963
μ (MoKα) / cm^{-1}	1.164	1.160	72.167
λ / Å	0.71075	0.71075	0.71075
$2\theta_{\mathrm{max}}$ / °	54.9	54.9	54.9
Reflections collected	5556	8081	8096
Unique reflections (R_{int})	899 (0.0312)	4390 (0.0280)	827 (0.0222)
Number of parameters	67	341	46
Final R_1 [$I > 2\sigma(I)$]	0.0275	0.0527	0.0249
wR_2 (all data)	0.0735	0.1300	0.0621
Goodness of fit	1.134	1.074	1.119
Residual electron density / Å^{-3}	0.26 e$^-$	0.38 e$^-$	1.72 e$^-$

References

S1. *CrystalClear*: *Data Collection and Processing Software*; Rigaku Corporation; Tokyo 196-8666, Japan, 1998-2014.

S2. Sheldrick, G. M. *Acta. Crystallogr. Sect. A* **2008**, *64*, 112-122.

S3. *CrystalStructure 4.1: Crystal Structure Analysis Package*; Rigaku Corporation; Tokyo 196-8666, Japan, 2000-2014.

S4. Speak, A. L. *Acta Crystallogr. Sect. C.* **2015**, *71*, 9-18.

S5. *Gaussian 09*, Revision D.01, M. J. Frisch, G. W. Trucks, H. B. Schlegel, G. E. Scuseria, M. A. Robb, J. R. Cheeseman, G. Scalmani, V. Barone, B. Mennucci, G. A. Petersson, H. Nakatsuji, M. Caricato, X. Li, H. P. Hratchian, A. F. Izmaylov, J. Bloino, G. Zheng, J. L. Sonnenberg, M. Hada, M. Ehara, K. Toyota, R. Fukuda, J. Hasegawa, M. Ishida, T. Nakajima, Y. Honda, O. Kitao, H. Nakai, T. Vreven, J. A. Montgomery, Jr., J. E. Peralta, F. Ogliaro, M. Bearpark, J. J. Heyd, E. Brothers, K. N. Kudin, V. N. Staroverov, T. Keith, R. Kobayashi, J. Normand, K. Raghavachari, A. Rendell, J. C. Burant, S. S. Iyengar, J. Tomasi, M. Cossi, N. Rega, J. M. Millam, M. Klene, J. E. Knox, J. B. Cross, V. Bakken, C. Adamo, J. Jaramillo, R. Gomperts, R. E. Stratmann, O. Yazyev, A. J. Austin, R. Cammi, C. Pomelli, J. W. Ochterski, R. L. Martin, K. Morokuma, V. G. Zakrzewski, G. A. Voth, P. Salvador, J. J. Dannenberg, S. Dapprich, A. D. Daniels, O. Farkas, J. B. Foresman, J. V. Ortiz, J. Cioslowski, and D. J. Fox, Gaussian, Inc., Wallingford CT, 2013.

S6. Zhu, X. –Z.; Chen, C. –F. *J. Org. Chem.* **2005**, 70, 917–924.